The Experimental Validation of Designed Fiber Optic Pressure Sensors With EPDM Diaphragm

Şekip Esat Hayber, Umut Aydemir, Timuçin Emre Tabaru, and Ömer Galip Saraçoğlu

***Abstract*— This paper focused on the experimental validation of diaphragm-based Fabry-Perot fiber optic pressure sensors (D-FP-FOPS) with ethylene propylene diene terpolymers (EPDM) diaphragm as designed and analyzed sensor tip theoretically. We also used self-adhesive EPDM rubber as a diaphragm for the first time in the literature. Analytical calculation and finite element method (FEM) analysis were carried out to obtain values of fundamental resonance frequency (f_0) and deflection (d) with diaphragm specific values of Young's modulus and Poisson's ratio measured by tensile tests. We produced D-FP-FOPS tip with EPDM diaphragm and obtained experimental f_0 between 250–400 Hz from extended signal to noise ratio (SNR) plot which figured out with the help of theoretical values of f_0. We also analyzed minimum detectable pressure (MDP) mapping which is used to confirm SNR mapping for D-FP-FOPS. We noticed that our sensor could be operated up to 1.6 Pa pressure which confirms the mechanical limit given in the literature. Before production of D-FP-FOPS, a pioneering way which includes design, analytical calculation, FEM analysis, and experimental validation was demonstrated as a novel. Moreover, since we used self-adhesive EPDM tape as a diaphragm material, our sensor tip cost is less than 50 $ which capable to compete with commercial sensors.**

***Index Terms*— Fiber optic sensor, design for experiments, pressure measurement, polymer films.**

I. Introduction

THE EARLY scientific studies on acoustic/pressure detection with fiber optic sensors are started in the 1970s [1], [2] and the number of scientific studies was increased due to their excellent advantages over classical sensors, such as electromagnetic immunity, high resolution, fast response, broadband range, robust durability solutions, lightweight, unlimited size and shape [3]. Recently, researchers have focused on diaphragm based Fabry-Perot (FP) interferometric sensors because they can provide to produce adjustable and ultra-sensitive sensors with various methods [4]. In literature, many scientific studies can be found a diaphragm-based FP fiber optic pressure sensor (D-FP-FOPS) including different diaphragm materials with different geometric dimension [5]–[8].

D-FP-FOPS has a wide variety of applications such as biomedical [9], temperate sensing [10], underwater [11], infrasound [12], non-destructive test [13], partial discharge [14], long distance listening and voice recognition [15] applications. The diaphragm material plays a crucial role in order to tune and increases device performance of D-FP- FOPSs. These diaphragm materials include metallic (Ag, Al, Au, etc.), silicon, silica, graphene, and polymers.

Last decade, different polymer films were used as a diaphragm material such as polyethylene terephthalate [16], SU-8 [17], polyimide [18], Parylene-C [19], polyvinyl chloride [20] in D-FP-FOPSs. Some polymers which used as a diaphragm are substantially limited in sensing applications due to their poor mechanical applications and instability in a different medium. Among them, ethylene propylene diene terpolymer (EPDM) is willing rubber with extended shelf-life, long-term performance, excellent resistance to oxygen, ozone, heat, and UV light, whereas the non-polar structure endows them with excellent electrical resistivity and resistance to polar solvents [21]. Therefore, it has extensive industrial applications to electrical insulation, building construction, automobile components, and aerospace applications [21]–[23]. Through its excellent mechanical properties, EPDM rubber is used as a diaphragm material for D-FP-FOPS in this article for the first time in the literature.

According to desired applications of D-FP-FOPSs, it also can be tuned by geometrical dimensions besides changing diaphragm materials. In literature, studies tend to miniaturization of D-FP-FOPS, and it can be produced by many time-consuming and expensive methods like microfabrication techniques, fusion splicers, the chemical process' and so forth. However, these methods remain unimportant when dimension limitations are not necessary. On the other hand, another disadvantageous of these techniques is that they cannot apply to low cost, fast, standard, and easy production [6], [14], [24]. Moreover, researchers should be theoretically simulated their designed devices before production to save time and cost.

In the present paper, we carried out a structural analysis of self-adhesive EPDM tape as diaphragm via Fourier transform infrared spectroscopy (FTIR) method. We also applied a tensile test to obtain the mechanical properties of our

Manuscript received March 8, 2019; accepted March 26, 2019. Date of publication April 1, 2019; date of current version June 19, 2019. This work was supported by the Research Funds for the TUBITAK under Grant 2170560. The associate editor coordinating the review of this paper and approving it for publication was Dr. Carlos Marques. *(Corresponding author: Umut Aydemir.)*

Ş. Esat Hayber is with the Department of Electronics and Automation, Kırşehir Ahi Evran University, 40300 Kırşehir, Turkey (e-mail: sehayber@ahievran.edu.tr).

U. Aydemir is with the Department of Electrical and Electronics Engineering, Uludag University, 16120 Bursa, Turkey (e-mail: umutaydemir@uludag.edu.tr).

T. E. Tabaru is with the Clinical Engineering Research and Application Center, Erciyes University, 38039 Kayseri, Turkey (e-mail: etabaru@erciyes.edu.tr).

Ö. G. Saraçoğlu is with the Department of Electrical and Electronics Engineering, Erciyes University, 38039 Kayseri, Turkey (e-mail: saracog@erciyes.edu.tr).

Digital Object Identifier 10.1109/JSEN.2019.2908410

EPDM tape. By using Young's modulus (E), Poisson's ratio (υ) and geometric dimensions (designed for FC adapter), precise analytical calculations of deflection and frequency response are obtained for EPDM diaphragm. Additionally, we also modeled EPDM diaphragm to determine same parameters by using finite element methods (FEM). We produced D-FP-FOPS with EPDM diaphragm to perform sensor analysis experimentally. We applied standard signal to noise ratio (SNR) measurements and extended SNR plot around fundamental resonance frequency (f_0) which is obtained from analytical and FEM results. In this way, we figured out f_0 peak around 362 Hz which hidden in standard SNR plot. The experimental results are perfect agreement with analytical calculation and FEM results. We also discussed the minimum detectable pressure (MDP) plot for sensor quality and voltage versus pressure relationship for sensor sensitivity. Before production of D-FP-FOPS, we followed design, analytical calculation, FEM analysis, and experimental validation steps, respectively by contributing to the literature. In this study, we used self-adhesive EPDM tape as a diaphragm material in sensor tip which total cost is less than 50 $.

II. Material and Methods

We used industrial self-adhesive EPDM tape as a diaphragm material. FTIR measurement of EPDM diaphragm was carried out between 500-4000 cm^{-1} with 1 cm^{-1} sensitivity by Perkin Elmer Spectrum400 spectrometer. Tensile tests were measured by Shimadzu AG-X Plus tensile testing system to define mechanical parameters of EPDM tape. The EPDM tape with dimensions of 44 mm length l, 19 mm width w and 50 μm thickness t is used for the mechanical test. The diaphragm specific values of E and υ obtained from the tensile test are used for analytical calculations and FEM analysis for determining deflection and frequency response of D-FP-FOPS. FEM analysis of diaphragm is carried out with the help of ANSYS software.

The schematic illustration of the experimental setup is depicted in Fig. 1 to measure sensor performance of D-FP-FOPS with EPDM diaphragm. We produced D-FP-FOPS tip with 4 mm radius, 50 μm thickness and same values are also used for analytical and FEM analysis. A laser diode with a wavelength of 1550 nm is used as a light source in the measurement setup (Ideal Fiber Master 33-929). 1525–1610 nm single mode fiber (SMF) with FC/PC (Thorlabs 6015-3-FC) is used as the circulator. A highspeed fiber-coupled InGaAs biased photodetector (Thorlabs DET08CFC-M, 5 GHz) is chosen to measure the reflected optical signal from the D-FP-FOPS tip. The photodetector responsivity is in the range of $800-1700$ nm, and the peak wavelength is 1550 nm. A PC oscilloscope and data logger measure the signals received from the detector (Picoscope 3206 MSO, 200 MHz analog bandwidth, 1 GS/s real-time sampling, 512 ms buffer memory). The sound level meter (SLM, IEC 61672-1 class 2) is used to check applied sound pressure. The PC oscilloscope also includes a spectrum analyzer, and the frequency domain measurements are carried out with this instrument. The spectrum analyzer in this instrument is of the fast fourier transform (FFT) type, which, unlike a conventional sweep spectrum analyzer, can display the spectrum of a single nonrepeatable waveform.

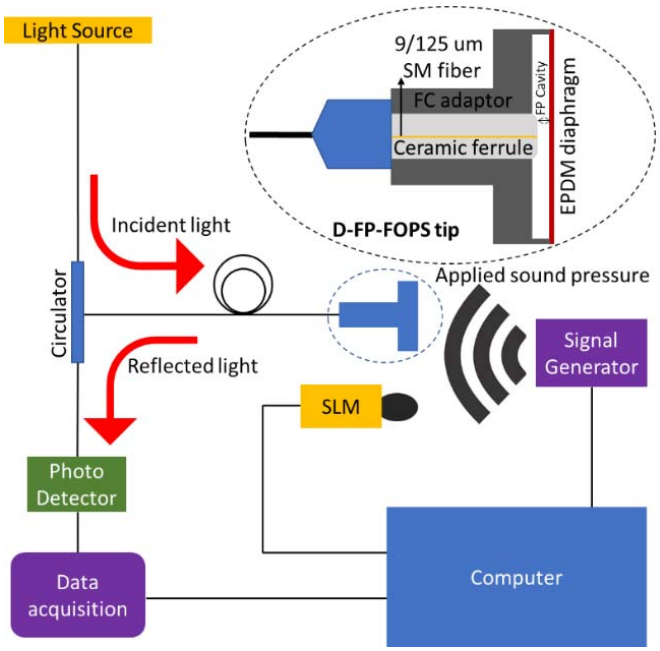

Fig. 1. Schematic illustration of the experimental setup for D-FP-FOPS with EPDM diaphragm.

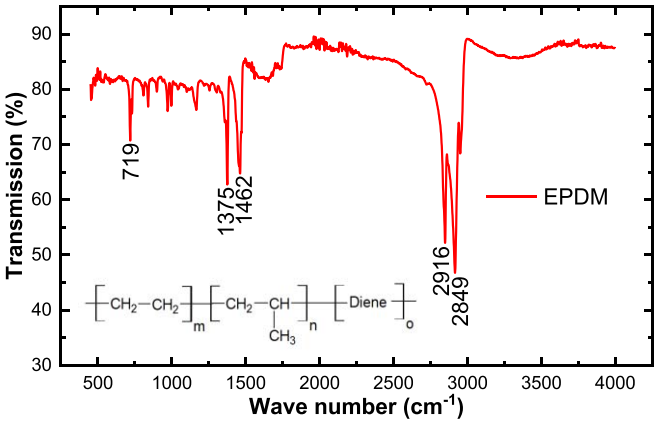

Fig. 2. FTIR spectrum of EPDM diaphragm.

III. Experimental Results and Discussion

A. Ftir Spectrum of Epdm Diaphragm

Infrared spectroscopy offers an opportunity comprehensive application analysis of molecular level and microstructure of polymers. According to Fig. 2, two main peaks at 2916, 2849 cm^{-1} correspond saturated hydrocarbon backbone of aliphatic alkyl symmetric/asymmetric C–H stretching for EPDM rubber [23]. The peaks at 1462, 1375 and 719 cm^{-1} indicate that deformation frequency of the same methylene groups refers as $-CH_2$ scissoring vibrations, $-CH_3$ bending and $(-CH_2)_n$ backbones where n is number of repeating unit of $(-CH_2)$ and $n \geq 5$, respectively. Its saturated backbone provides exceptional resistance to severe ambient conditions. Experimental results are good agreement with FTIR results

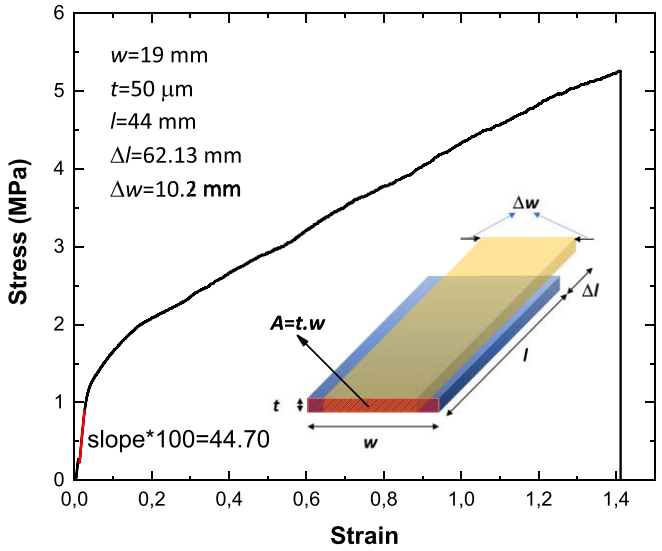

Fig. 3. Stress versus strain plot of EPDM film.

published in the literature [23], [25]. Technical parameters of EPDM can be found with CAS number of 25038-36-2.

B. Tensile Test and Modelling

Before production of D-FP-FOPS with EPDM diaphragm, we applied tensile test on EPDM tape. As can be seen in Fig. 3, we calculated the diaphragm specific value of E from stress (F/A) versus strain $(\Delta l/l)$ plot in elastic region for EPDM as 44.7 MPa with following equation [26];

$$E = \frac{F/A}{\Delta l/l}. \tag{1}$$

where F is force, A is cross sectional area, Δl is the amount by which the length of the object changes and l is length of EPDM. Strain-stress plot bends after strain of 5% and enters the plastic region and breaks at 141% strain. We also calculate Poisson's ratio (υ) of EPDM as 0.38 elongation at break with the following equation [26];

$$\upsilon = \frac{\Delta w/w}{\Delta l/l}. \tag{2}$$

where Δw is the amount by which the width of the object changes and w is width of EPDM.

Load-deflection method is a well-known method to calculate of deflection of the diaphragm. When the applied pressure changes, the diaphragm is deformed accordingly. Because the diaphragm is flat and of uniform thickness, its center deflection d, under applied pressure P, can be calculated by [27];

$$d = \frac{3\left(1-\upsilon^2\right)P}{16Et^3}r^4. \tag{3}$$

In addition to the consideration for diaphragm sensitivity (deflection/pressure), the diaphragm frequency response is another important issue. We define the diaphragm as a free vibrating circular plate clamped rigidly at the edge. Its fundamental resonance frequency f_0 is expressed

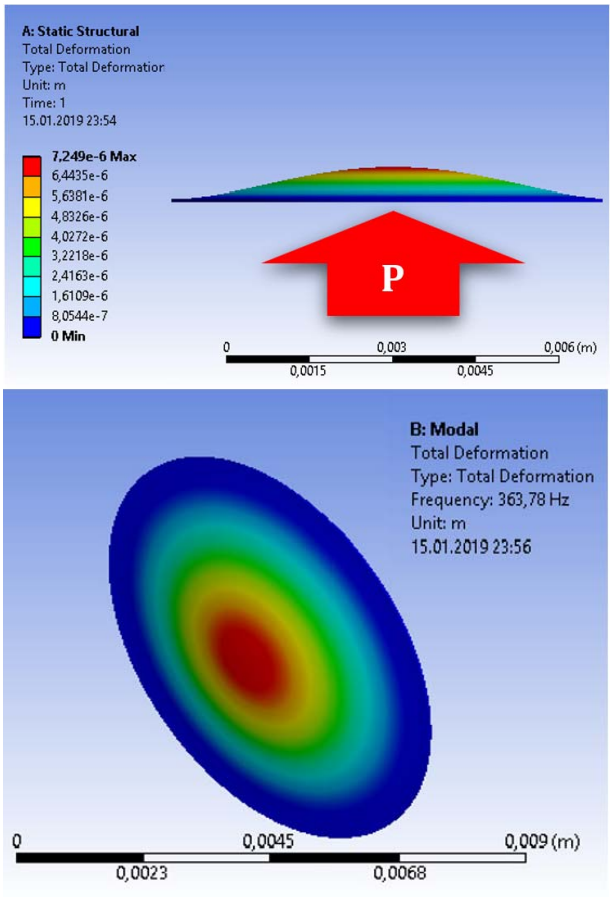

Fig. 4. (a) Static structural, and (b) modal analysis of EPDM diaphragm.

follows [27];

$$f_0 = \frac{10.21}{2\pi r^2}\sqrt{\frac{Et^2}{12\rho\left(1-\upsilon^2\right)}}. \tag{4}$$

Where υ is Poisson's ratio, E is Young's modulus, ρ is the mass density, r is the radius, and t is a thickness with values of 0.38, 44.7 MPa, 860 kg/m^3, 4 mm and 50 μm for the EPDM diaphragm, respectively. It is easy to calculate d and f_0 of the diaphragm under an acoustic/pressure value of P respectively from (3), and (4). Unidentified values of E and υ causes a significant discrepancy between theoretical and experimental results of the sensor. In our proposed way, precise analytical calculations may be obtained with diaphragm specific E and υ values which are very important for sensor designers. After that, we analytically calculated f_0 with the value of 361 Hz and d with the value of 7.4 μm/Pa for EPDM diaphragm.

As can be shown in Fig. 4(a) and Fig. 4(b), FEM simulation was performed by using static structural analysis for d and modal analysis for f_0, with values of 7.3 μm/Pa and 364 Hz, respectively.

C. Experimental Validation

As seen in Fig. 5(a), we measured the standard SNR plot between 500 Hz to 20 kHz with 500 Hz sensitivity after production of D-FP-FOPS. Researchers, scan SNR data

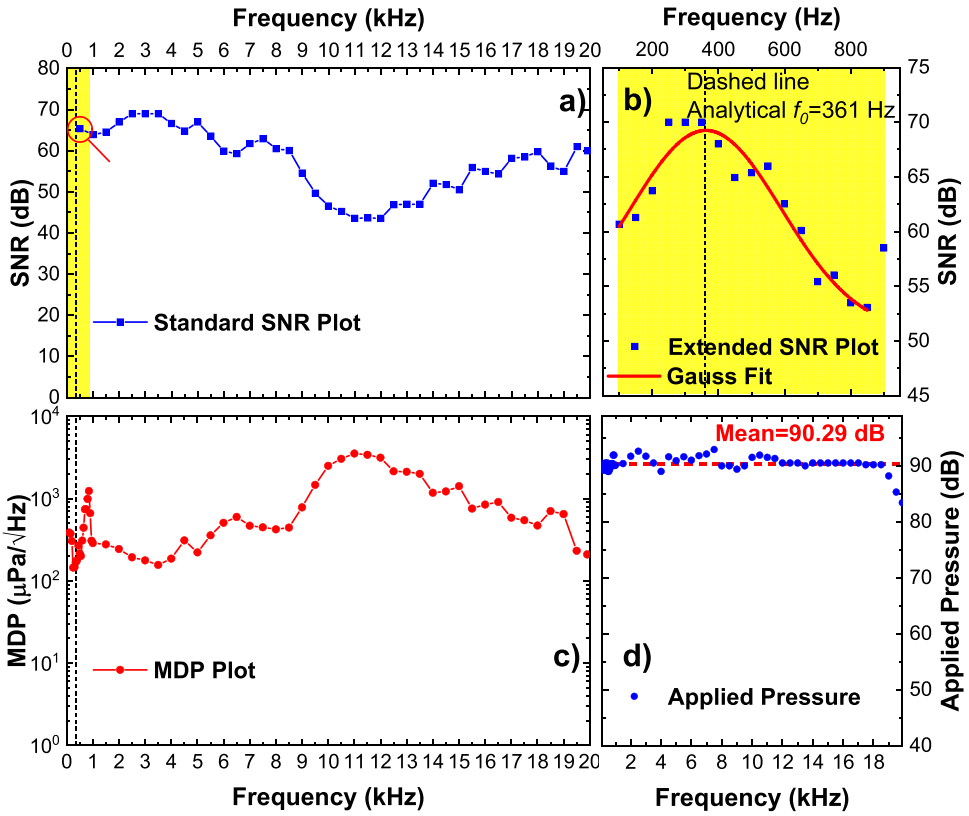

Fig. 5. Frequency dependent (a) standard SNR plot, (b) extended SNR plot, (c) MDP plot, and (d) applied pressure plots.

with increasing frequency by a constant frequency step after production of sensor tip without any prediction about the sensor. SNR plot is a significant parameter to understand sensor sensitivity and bandwidth, and it should be supported by theoretical f_0 value. As given in Fig. 5(b), we extended SNR plot around analytical f_0 which indicated dashed line at 361 Hz in Fig. 5(b) for D-FP-FOPS with EPDM diaphragm and discovered a peak, via Gauss fit, which hidden in standard SNR plot as given in Fig. 5(a) which contributes literature. Usually, it should be noted that SNR has a maximum value between 2.5-3.5 kHz frequencies. Since we increased sensitivity by 50 Hz step between 100-900 Hz, we did not make a mistake in standard SNR plot in Fig. 5(a). Without prediction of f_0 obtained from analytical calculations or FEM analysis, it is hard to figure out f_0 of the sensor in SNR plot. The reason to avoid researchers' theoretical analyses before production of D-FP-FOPS is indefinite specific values of E and υ of their diaphragm material. As a result, literature suffers from the validation of a theoretical and experimental comparison of D-FP-FOPS. By using specific values of E and υ of EPDM diaphragm, 361 Hz obtained from the analytical calculation, 364 Hz obtained from FEM analysis and, 250-400 Hz obtained from experimental values of f_0 which are in good agreement with each other. In this way, we validate theoretical results with experimental results as a novel for D-FP-FOPS with EPDM diaphragm. MDP is another critical parameter for D-FP-FOPS. As shown in Fig. 5(c), MDP value has a minimum value around f_0 and reaches maximum value around minimum SNR value. Additionally, there is a linear proportion

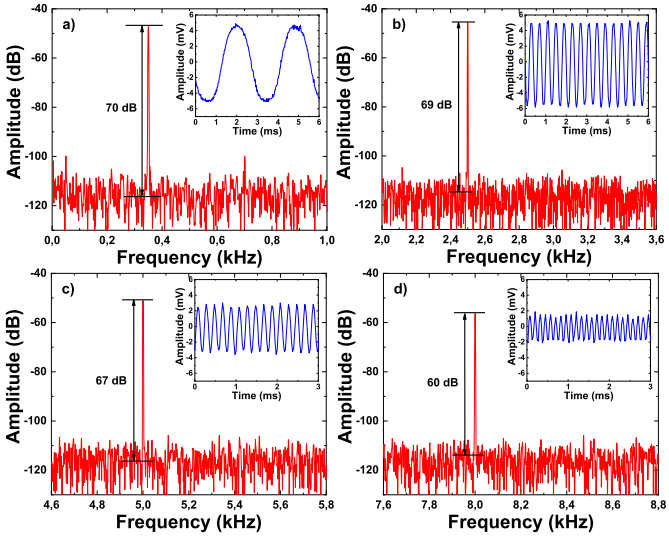

Fig. 6. SNR values at different frequencies (a) 0.35, (b) 2.5, (c) 5, and (d) 8 kHz.

between applied pressure and signal output. Hence as can be seen in Fig. 5(d), these measurements were recorded under regularly applied pressure (Mean 90.29 dB) to ensure exact SNR and MDP plots. As a result of experiments under constant pressure, SNR plot is a reflection by x-axis of MDP plot which we called as mirror effect.

The frequency domain plots are given in Fig. 6 which contains 0.35, 2.5, 5, and 8 kHz and inset figures are also

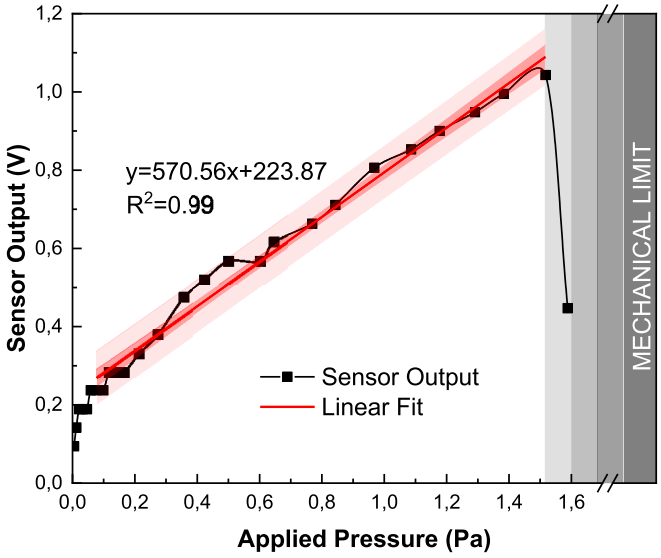

Fig. 7. Applied pressure versus sensor output.

TABLE I
SUMMARY OF THE OBTAINED PARAMETERS OF D-FP-FOPS WITH EPDM DIAPHRAGM

Method	E (MPa)	v	f_0 (Hz)	d (μm)	SL (Pa)
Analytic	-	-	361	7.35	2.04
FEM	-	-	364	7.25	2.06
Exp.	44.70	0.38	250-400	-	1.6

given in time domain for each frequency. Although we try to apply constant pressure to D-FP-FOPS, a small deviation occurs during the experiment. We applied 90.5, 92.6, 90.9, and 90 dB acoustic pressure and measure SNR values as 70, 69, 67, and 60 dB at 0.35, 2.5, 5, and 8 kHz, respectively. It is confirmed that we applied 90.5 dB and measured the maximum SNR value of 70 dB at 350 Hz (around f_0) when we compared the SNR values of other frequencies. Bandutunga *et al.* produced their sensor tip with polyethylene terephthalate polymer diaphragm (PETP) diaphragm and they observed SNR and MDP values as 47 dB with 1 Pa and 74 μPa/$\sqrt{}$Hz at 1 kHz, respectively [16]. Wang and Yu measured a SNR value of 29 dB, by using a poly (phthalazinone ether sulfone ketone) (PPESK) diaphragm for acoustic sensing [5]. While we apply 0.6 Pa acoustic pressure to D-FP-FOPS with EPDM diaphragm, we measured SNR value as 70 dB at 0.35 kHz and these results confirm sensitivity of our sensor.

Equation (3) which we used to calculate the deflection of diaphragm above is valid in mechanical limits. A D-FP-FOPS works in a linear region when center deflection of the diaphragm is less than 30% of the diaphragm thickness. It is named as the mechanical limit, and we observed our mechanical limit is 15 μm for the deflection or 2 Pa pressure. As seen in Fig. 7, there is a linear relationship between the sensor output voltage and the applied pressure. Even applied pressure does not reach the mechanical limit; the sensor output is drastically decreasing with pressure over 1.6 Pa. These results confirm mechanical limit, and D-FP-FOPS with EPDM diaphragm can be operated up to 1.6 Pa pressure which is called sensor limit (SL). Our sensor output has a linear response between 0.1-1.5 Pa, and system sensitivity is observed as 794 mV/Pa. Wang and Yu also reported their sensitivity as 31 mV/Pa for fiber optic sensor with PPESK diaphragm [5]. All sensor parameters are given in Table 1 as for comparison.

IV. CONCLUSION

In conclusion, since we used EPDM tape, we measured FTIR spectrum for structural analysis. In order to define diaphragm specific Young's modulus and Poisson's ratio, we applied the mechanical test on EPDM tape. After determining specific values of E and v, we designed our D-FP-FOPS with EPDM diaphragm and analyzed f_0 and d by analytical and FEM analysis first. After obtaining of f_0 and d, we produced D-FP-FOPS tip with EPDM diaphragm and drew SNR and MDP plots to understand sensor performance. Since we know f_0 around 360 Hz obtained from theoretically, we extended the standard SNR plot between 100-900 Hz with 50 Hz steps. We revealed the peak of experimental f_0 between 250-400 Hz which hidden in standard SNR plot. In this way, we confirmed designed D-FP-FOPS with EPDM diaphragm with the help of analytical, FEM and experimental results. MDP plot, another important parameter of sensors, is observed. MDP plot looks like a good reflection by x-axis of SNR plot due to the correct response of sensor output measured under a constant pressure around 90 dB. Our produced D-FP-FOPS with EPDM diaphragm has a maximum operating limit of 1.6 Pa which closes to the mechanical limit.

Contrary to the literature before production of D-FP-FOPS, we step by step carried out design, analytical calculations, FEM analysis, an experimental validation, respectively. Similar design operations performed before the sensor diaphragm is manufactured will facilitate and accelerate the process to produce sensors with the desired operating ranges. This study is a candidate to be a helpful guide for researchers who design, analysis and validate D-FP-FOPS.

REFERENCES

[1] J. H. Cole, R. L. Johnson, and P. G. Bhuta, "Fiber-optic detection of sound," *J. Acoust. Soc. Amer.*, vol. 62, no. 5, pp. 1136–1138, Aug. 1977.
[2] J. A. Bucaro, H. D. Dardy, and E. F. Carome, "Optical fiber acoustic sensor," *Appl. Opt.*, vol. 16, no. 7, pp. 1761–1762, 1977.
[3] Y. J. Rao, "Recent progress in fiber-optic extrinsic Fabry–Pérot interferometric sensors," *Opt. Fiber Technol.*, vol. 12, no. 3, pp. 227–237, Jul. 2006.
[4] M. R. Islam, M. M. Ali, M. H. Lai, K. S. Lim, and H. Ahmad, "Chronology of Fabry–Pérot interferometer fiber-optic sensors and their applications: A review," *Sensors*, vol. 14, no. 4, pp. 7451–7488, Apr. 2014.
[5] Q. Wang and Q. Yu, "Polymer diaphragm based sensitive fiber optic Fabry–Pérot acoustic sensor," *Chin. Opt. Lett.*, vol. 8, no. 3, pp. 266–269, 2010.
[6] W. Ni *et al.*, "Ultrathin graphene diaphragm-based extrinsic Fabry–Pérot interferometer for ultra-wideband fiber optic acoustic sensing," *Opt. Express*, vol. 26, no. 16, pp. 20758–20767, 2018.
[7] J. Eom, C.-J. Park, B. H. Lee, J. H. Lee, I.-B. Kwon, and E. Chung, "Fiber optic Fabry–Pérot pressure sensor based on lensed fiber and polymeric diaphragm," *Sens. Actuators A, Phys.*, vol. 225, no. 1, pp. 25–32, Apr. 2015.

[8] X. Wang, J. Xu, Y. Zhu, K. L. Cooper, and A. Wang, "All-fused-silica miniature optical fiber tip pressure sensor," *Opt. Lett.*, vol. 31, no. 7, pp. 885–887, 2006.
[9] P. Roriz, O. Frazão, A. B. Lobo-Ribeiro, J. L. Santos, and J. A. Simões, "Review of fiber-optic pressure sensors for biomedical and biomechanical applications," *J. Biomed. Opt.*, vol. 18, no. 5, May 2013, Art. no. 050903.
[10] J. Yin *et al.*, "Batch-producible fiber-optic Fabry–Pérot sensor for simultaneous pressure and temperature sensing," *IEEE Photon. Technol. Lett.*, vol. 26, no. 20, pp. 2070–2073, Oct. 15, 2014.
[11] D. B. Duraibabu *et al.*, "An optical fibre depth (pressure) sensor for remote operated vehicles in underwater applications," *Sensors*, vol. 17, no. 2, p. 406, Feb. 2017.
[12] S. Wang *et al.*, "An infrasound sensor based on extrinsic fiber-optic Fabry–Pérot interferometer structure," *IEEE Photon. Technol. Lett.*, vol. 28, no. 11, pp. 1264–1267, Jun. 1, 2016.
[13] C. Li, X. Peng, Q. Liu, X. Gan, R. Lv, and S. Fan, "Nondestructive and *in situ* determination of graphene layers using optical fiber Fabry–Pérot interference," *Meas. Sci. Technol.*, vol. 28, no. 2, Jan. 2017, Art. no. 025206.
[14] W. Si, C. Fu, D. Li, H. Li, P. Yuan, and Y. Yu, "Directional sensitivity of a MEMS-based fiber-optic extrinsic Fabry–Pérot ultrasonic sensor for partial discharge detection," *Sensors*, vol. 18, no. 6, p. 1975, 2018.
[15] S. E. Hayber, T. E. Tabaru, S. Keser, and O. G. Saracoglu, "A simple, high sensitive fiber optic microphone based on cellulose triacetate diaphragm," *J. Lightw. Technol.*, vol. 36, no. 23, pp. 5650–5655, Dec. 1, 2018.
[16] C. P. Bandutunga, R. Fleddermann, M. B. Gray, J. D. Close, and J. H. Chow, "All-optical low noise fiber Bragg grating microphone," *Appl. Opt.*, vol. 55, no. 21, pp. 5570–5574, 2016.
[17] J. Wu, M. Yao, F. Xiong, A. P. Zhang, H. Y. Tam, and P. K. A. Wai, "Optical fiber-tip Fabry-Pérot interferometric pressure sensor based on an *in-situ* μ-printed air Cavity," *J. Lightw. Technol.*, vol. 36, no. 17, pp. 3618–3623, Sep. 1, 2018.
[18] Y. Zhao, Y. Yuan, W. Gan, and M. Yang, "Optical fiber Fabry–Pérot humidity sensor based on polyimide membrane: Sensitivity and adsorption kinetics," *Sens. Actuators A, Phys.*, vol. 281, no. 1, pp. 48–54, Oct. 2018.
[19] Z. Gong, K. Chen, Y. Yang, X. Zhou, and Q. Yu, "Photoacoustic spectroscopy based multi-gas detection using high-sensitivity fiber-optic low-frequency acoustic sensor," *Sens. Actuators B, Chem.*, vol. 260, no. 1, pp. 357–363, May 2018.
[20] Z. Zhang *et al.*, "High-sensitivity gas-pressure sensor based on fiber-tip PVC diaphragm Fabry-Pérot interferometer," *J. Lightw. Technol.*, vol. 35, no. 18, pp. 4067–4071, Sep. 15, 2017.
[21] J.-R. R. Ruiz, T. Canals, and R. Cantero, "Supervision of ethylene propylene diene M-class (EPDM) rubber vulcanization and recovery processes using attenuated total reflection Fourier transform infrared (ATR FT-IR) spectroscopy and multivariate analysis," *Appl. Spectrosc.*, vol. 71, no. 1, pp. 141–151, Jan. 2017.
[22] H. Zhang, R. N. Datta, A. G. Talma, and J. W. Noordermeer, "Maleic-anhydride grafted EPM as compatibilising agent in NR/BR/EPDM blends," *Eur. Polym. J.*, vol. 46, no. 4, pp. 754–766, Apr. 2010.
[23] S. Gunasekaran, R. K. Natarajan, and A. Kala, "FTIR spectra and mechanical strength analysis of some selected rubber derivatives," *Spectrochimica Acta A, Mol. Biomol. Spectrosc.*, vol. 68, no. 2, pp. 323–330, Oct. 2007.
[24] Y. Wu *et al.*, "A highly sensitive fiber-optic microphone based on graphene oxide membrane," *J. Lightw. Technol.*, vol. 35, no. 19, pp. 4344–4349, Oct. 1, 2017.
[25] A. I. Hussain, M. L. Tawfic, A. A. Khalil, and T. E. Awad, "High performance emulsified EPDM grafted with vinyl acetate as compatibilizer for EPDM with polar rubber," *Nature Sci.*, vol. 8, no. 10, pp. 348–357, 2010.
[26] J. R. Davis, (Ed.), *Tensile Testing*. Materials Park, OH, USA: ASM International, 2004.
[27] J. Xu, X. Wang, K. L. Cooper, and A. Wang, "Miniature all-silica fiber optic pressure and acoustic sensors," *Opt. Lett.*, vol. 30, no. 24, pp. 3269–3271, 2005.

Şekip Esat Hayber received the M.S. and Ph.D. degrees from the Department of Electrical-Electronics Engineering, Erciyes University, Kayseri, Turkey, in 2011 and 2018, respectively.

He is working as a Researcher with the Department of Electronic and Automation, Kırşehir Ahi Evran University, Turkey. His research involves optic and fiber optic detection, optical fiber sensing system, and photonic sensors.

Umut Aydemir received the M.S. and Ph.D. degrees from the Department of Physics, Faculty of Arts and Sciences, Gazi University, Ankara, Turkey, in 2010 and 2015, respectively.

He is working as an Assistant Professor with the Department of Electrical and Electronics Engineering, Uludag University, Turkey. His research areas involve semiconductor devices, single crystal growth layered crystals, and nanophotonic and nanoelectronic devices.

Timuçin Emre Tabaru received the M.S. and Ph.D. degrees from the Department of Electrical-Electronics Engineering, Erciyes University, Kayseri, Turkey, in 2014 and 2018, respectively.

He is working as a Lecturer with The Clinical Engineering Research and Application Center, Erciyes University. His current research interests are fiber optic sensors, optical signal processing, photoacoustic detection, photonic sensors, biomedical optics, and electro-optical instruments.

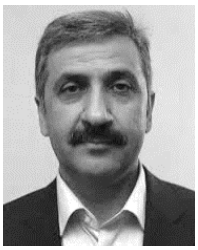

Ömer Galip Saraçoğlu received the M.S. and Ph.D. degrees in electronics engineering from Erciyes University, Turkey, in 1995 and 2000, respectively.

He is a full-time Professor with the Department of Electrical and Electronics Engineering, Erciyes University. His current research interests include optoelectronic materials and devices, photonic sensors, biomedical optics, metamaterials, and electromagnetic compatibility.